

# The Effect of SiC Particle Addition During FSW on Microstructure and Mechanical Properties of AZ31 Magnesium Alloy

M. Abbasi, A. Abdollahzadeh, B. Bagheri, and H. Omidvar

(Submitted April 16, 2015; in revised form October 14, 2015; published online November 2, 2015)

Welding and joining of magnesium alloys exert a profound effect on magnesium application expansion, especially in ground and air transportations where large-size, complex components are required. Due to specific physical properties of magnesium, its welding requires great control. In general, the solid-state nature of friction stir welding (FSW) process has been found to produce a low concentration of defects. In the current research, specimens from AZ31 magnesium alloy were welded together using the friction stir process with previously inserted SiC powder particles in the nugget zone. In other words, during the FSW process, the pre-placed SiC particles were stirred throughout the nugget zone of the weld. The results indicated that proper values of rotation and translation speeds led to good appearance of weld zone and suitable distribution of SiC particles producing increased weld strength. The comparison of the microstructures and mechanical properties of FS-welded AZ31 with those of FS-welded one using pre-placed SiC particles showed that the addition of SiC particles decreased the grain size and increased the strength and the formability index.

**Keywords** AZ31 magnesium alloy, friction stir welding, SiC particles

## 1. Introduction

Magnesium is the sixth most abundant element on the Earth's surface, with virtually inexhaustible supplies in the oceans (Ref 1). Magnesium alloys and especially AZ31 represent unique structural materials combining low density and high specific strength with the capability to absorb shock and vibration energy (Ref 2). AZ31 finds application in a wide variety of uses including aircraft fuselages, cell phone and laptop cases, speaker cones, concrete tools, and automotive components (Ref 3). The principal drawbacks of Mg alloy as a structural material when fusion welded are residual stresses, metallurgical structure change, contamination, and porosity (Ref 4).

Presently, solid-state joining techniques like friction welding and friction stir welding are widely accepted as alternative joining methods for welding of magnesium and its alloys (Ref 5). Friction stir welding is a solid-state welding process which uses friction as its main source to form welding. A rotating tool with a pin and a shoulder is longitudinally fed at a constant rate into a butt joint between two clamped pieces of material. The friction between the shoulder and the material produces enough heat to plasticize the material, and the pin helps move the plasticized material to form a strong bond between the materials to be joined (Ref 6). Even though the joints made by FSW

show better mechanical properties than the fusion-welded joints, research has been carried out to improve the different characteristics of these joints. Post weld heat treatment and change of chemical composition of the weld nugget are some of these attempts.

Retrospection and re-aging (RRA) as a specially developed heat treatment was applied by Kumar et al. (Ref 7) to improve the corrosion resistance of FS-welded AA7075 alloys. Friction stir welding of AA7075 alloy with the addition of boron carbide ( $B_4C$ ) powder resulted in an improvement in the hardness of weld nugget, and it was attributed to the uniform distribution of strengthening precipitates in the matrix and particle strengthening. According to Huang et al. (Ref 8), AZ31 Mg alloy reinforced with SiC particles using friction stir processing revealed that the pinning effect of SiC particles retarded the grain growth and increased the hardness (Ref 8).

Zhan et al. (Ref 9) investigated the feasibility of FSW in joining AZ31 magnesium alloy and studied the microstructures of FS-welded specimens. They obtained low-distortion, high-strength, and crack-free joints using FSW. They did not find new phase in the weld nugget, but observed high density of dislocations in this region. Karthikeyan and Mahdevan (Ref 10) studied the effects of SiC particle addition in the weld zone during FSW of AA6351 alloy. SiC particles were applied to the welding edges of the AA6351 alloy plates prior to welding for introduction and incorporation of SiC particles in the weld region. The results indicated that the addition of SiC particles restricts the grain boundary growth by pinning and resulted in an increase in the mechanical properties to an extent of 33% in the as-welded condition over plain alloy. SiC particles with a mean size of 5  $\mu m$  were introduced into the FSW of pure copper joints with the purpose to improve the mechanical properties of the Cu joints (Ref 11). The SiC particles were inserted into the 1-mm-wide gap between the two adjoining plates clamped together and then FSW was carried out. It was

M. Abbasi, Faculty of Engineering, University of Kashan, Kashan, Iran; and A. Abdollahzadeh, B. Bagheri, and H. Omidvar, Department of Mining and Metallurgy, Amirkabir University of Technology, Tehran, Iran. Contact e-mail: m.abbasi@aut.ac.ir.

found that the SiC particles stimulated nucleation in the dynamic recrystallization of Cu during the FSW process, and consequently the grain structure was refined and the hardness increased.

In the current research, SiC particles were introduced into the nugget zone of FS-welded AZ31 Mg alloy to improve the microstructure and mechanical properties. Particles were incorporated in the microstructure, and consequently a metal matrix composite reinforced by the particles was formed in the stir zone. The effect of FSW parameters, namely rotation and traverse speeds, on microstructure and mechanical properties of FS-welded and processed samples was investigated. The optimum values for welding were obtained based on trial-and-error method. Microstructure and mechanical properties of the optimum weld were evaluated and compared with those of the FS-welded sample without SiC addition.

## 2. Materials and Methods

AZ31 magnesium alloy with a nominal composition of 2.82 mass%Al, 0.94 mass%Zn, 0.42 mass%Mn, 0.023 mass%Ca, 0.011 mass%Cu, 0.03 mass% other elements, and Mg as a balance was used as a base material. For the FSW process, two AZ31 Mg alloy specimens with 6 mm thickness, 200 mm length, and 50 mm width were clamped together in a butt position in the fixture. SiC particles with a mean size of 55  $\mu\text{m}$  were inserted into the groove formed by machining between the joining specimens. A schematic of the groove between two joining specimens is depicted in Fig. 1(a). The specimen clamped in fixture is shown in Fig. 1(b). 0.7 g of SiC particles were placed in the groove before welding.

The FSW tool was made of H13 steel. The pin had a tapered cylindrical shape. The dimensions of pin and shoulder are presented in Table 1. Different trials were carried out. Rotation and traverse speeds are varied in the range noted in Table 1.

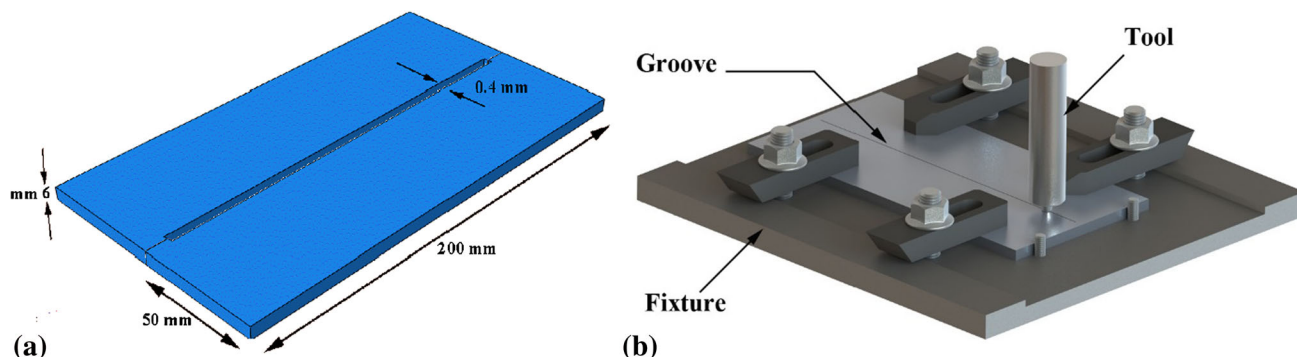


**Fig. 1** (a) Design of groove machined on specimens before welding in order to be filled by powders and (b) the arrangement of specimens in fixture

**Table 1** Values of FSW process parameters and the dimensions of pin and shoulder

Rotation speed, rpm	Traverse speed, mm/min	Tilt angle, °C	Shoulder diameter, mm	Pin height, mm	Top diameter of pin, mm	Bellow diameter of pin, mm
600-800-1000	25-75-125-175	3	20	5.8	7.2	5.1

Metallographic samples were prepared from the transverse section of the processed specimens. Sample preparation included grinding, polishing, and etching. Metallographic samples were etched for 1-2 s with an etchant consisted of 4.2 g picric acid, 10 ml acetic acid, 10 ml water, and 70 ml ethanol.

The distribution of the SiC particles was observed by SEM (JEOL JSM-6460LA), and the grain size of the etched sample was evaluated by optical microscopy. The grain size was quantified through the mean linear intercept method [ASTM E-112 (Ref 12)].

To measure the grain size, a rectangle of selected area ( $100 \times 100 \mu\text{m}^2$ ) was overlaid on a micrograph and the number of grains, consisting of the grains completely within the known area plus one half of the number of grains intersected by the circumference of the area, was counted. Accordingly, the number of grains per unit area was calculated, and then the average diameter of grains in the field was estimated assuming the grains to be spherical in shape. The grain size measurement for each sample was conducted on three different fields. Standard deviation of mean grain size for sample FS welded and processed with SiC particles was 0.7  $\mu\text{m}$  and for FS-welded specimen was 1.3  $\mu\text{m}$ .

After welding, subsize tensile test samples were prepared according to ASTM-E8 standard test (Ref 13). The samples were obtained from the welded specimens using the electrical discharge machine. The schematic design of tensile test sample is presented in Fig. 2. For each welding condition, three samples were tested. During the tests, the strain rate was 5 mm/min.

Vickers microhardness tester based on ASTM-E348 standard test (Ref 14) was used for evaluation of hardness. The applied load was 25 gf and dwell time was 10 s. Three samples for each welding condition were tested. Hardness of three points in nugget zone of each sample was measured. The distance between hardness measured points was 1 mm. Standard deviation for hardness measurement was 3.4 HV.

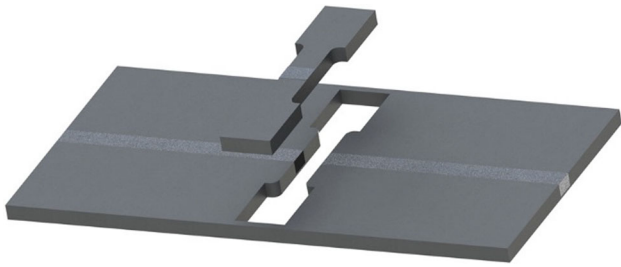
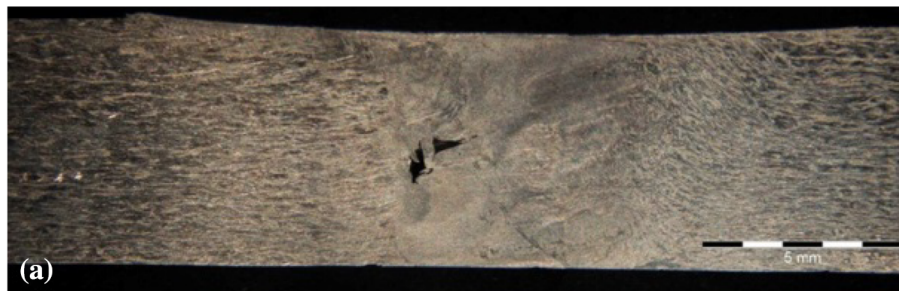


**Fig. 2** Schematic design of subsize tensile test samples obtained from FS-welded specimens using wire cut

### 3. Results and Discussion

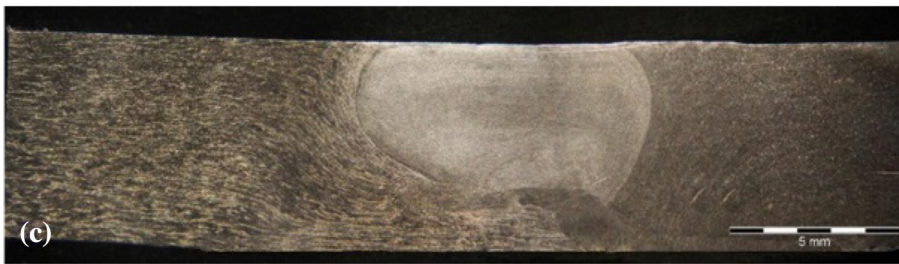
Different trials of FSW process with the addition of SiC particles according to Table 1 were carried out. The macrostructure of some FS-welded specimens, for different welding conditions, are presented in Fig. 3. The formation of voids and cavities, non-homogenous distribution of particles as well as incomplete stirring of material in nugget zone were some deficiencies that occurred during FSW process with the addition of SiC particles (Fig. 3). Macrostructure of a proper sample is also presented in Fig. 3(d). None of the listed problems are observed in Fig. 3(d). These results indicate that



w=600 rpm, v=25 mm/min



w=600 rpm, v=75 mm/min



w=1000 rpm, v=25 mm/min



w=800 rpm, v=125 mm/min

**Fig. 3** Macrostructure of some samples which are FS welded and processed with SiC particles: (a) formation of cavity, (b) non-homogenous distribution of SiC particles, (c) incomplete stirring of material in nugget zone, and (d) fair macrostructure (w and v stand for rotation and transverse speeds, respectively)

welding conditions have great influence on the developed macrostructure.

Non-homogenous distribution of SiC particles in weld zone which is a consequence of improper welding conditions is compared with homogenous distribution in Fig. 4. It is observed that for the first sample, the particle sizes are small and the particles are distributed homogeneously, while for the second sample the particles with large size are distributed non-homogeneously. It should be noted that the SiC powder size, applied in experiments, was about 45-65 nm, but due to agglomeration of powders which occurs during stirring, the size of particles in Fig. 4 is greater than 65 nm. EDS analyses for two points, SiC-rich (point A in Fig. 4b) and SiC-poor (point B in Fig. 4b) points, are presented in Fig. 5. It is seen that Mg and Si peaks are characteristics of SiC-rich zones and Si peak for SiC-poor zones is not significant.

The effect of rotational and traverse speeds of shoulder on grain size and mechanical properties of the sample FS welded and processed by SiC particles was investigated. The results are presented in Fig. 6. It is observed that there are optimum values for these parameters which result in maximum strength and ductility and minimum grain size.

The authors believe that two variables are affective on microstructure and mechanical properties of the studied samples, the generated heat during friction stirring and the presence of SiC particles. While the former leads to grain growth, the latter inhibits it. According to the model presented by Ashby (Ref 15), the presence of second-phase particles results in the creation of dislocation loops and dislocation cell structure around the particles during deformation and consequently the grain size decreases. Abbasi et al. (Ref 16) noted that the decrease of traverse speed and/or the increase of the rotational

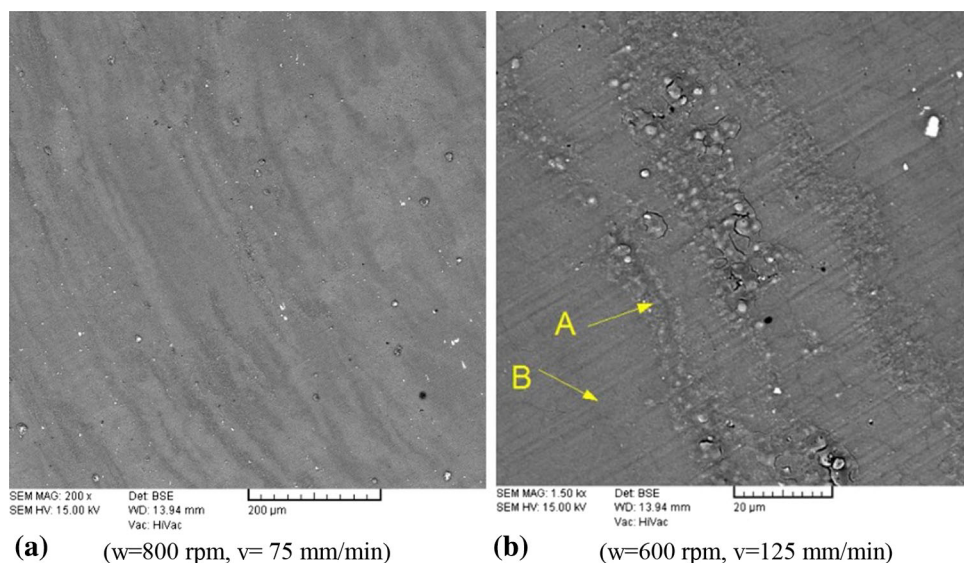


**Fig. 4** SEM pictures of two samples (a) FS welded and processed with SiC particles while the distribution is homogenous, and (b) FS welded and processed with SiC particles while the distribution is non-homogenous (A and B denote the SiC-rich and SiC-poor regions, respectively) (w and v stand for rotation and traverse speeds, respectively.)

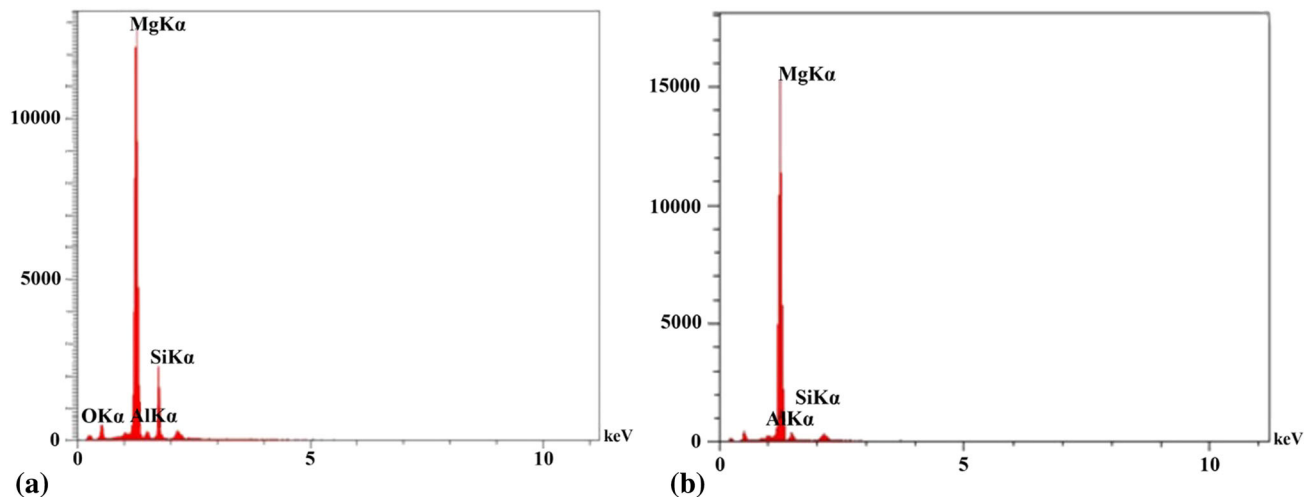


**Fig. 5** EDS peaks of (a) SiC-rich region and (b) SiC-poor region. SiC-rich and SiC-poor regions are denoted in Fig. 4 with A and B, respectively

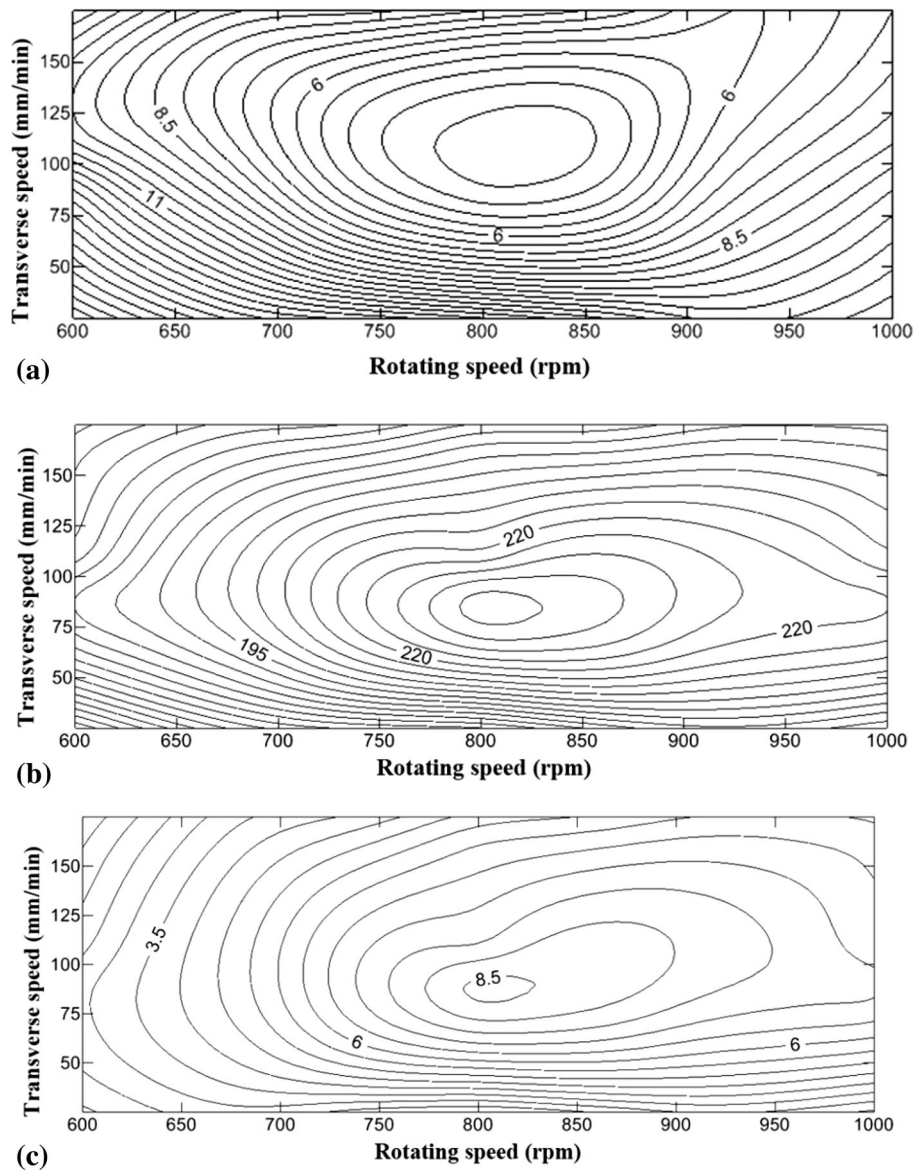


**Fig. 6** Effect of rotational and traverse speeds on different characteristics of FS-welded and processed samples: (a) grain size, (b) ultimate tensile strength, and (c) ductility

speed during FSW result in the enhancement of temperature and grain size in the weld zone and correspondingly decrease the strength. In the case of FSW with the addition of SiC particles, it is believed that when generated heat during FSW is high, the stirring effect is complete. In this condition, although the grains can grow readily, the SiC particles may distribute homogeneously and interparticle spacing is low. So, heat input and SiC particles have opposite effects on the grain size. In Fig. 7, microstructures of some FS-welded and processed samples are shown. These microstructures relate to various welding conditions. In Fig. 7, as the heat input to the weld region increases, the grain size increases and the SiC particles are distributed more homogeneously.

Figure 7b indicates that low heat input to the weld region results in a lack of proper stirring and non-homogeneous distribution of SiC particles while interparticle spacing is high. In this condition, the grain size of weld region does not differ considerably from the base material. In Fig. 8, the relation

between FSW parameters and the temperature of the weld zone which is representative of the heat generated in the weld zone is presented schematically. Additionally, the resultant effects of temperature on grain size and interparticle spacing are shown schematically.

The results in Fig. 6(b) and (c) indicate that neither high rotation and low traverse speeds nor low rotation and high traverse speeds do not guarantee the highest strength and ductility. This result can also be explained differently by Hall-Petch and Orowan-Ashby equations (Ref 17). These equations can be utilized to justify the effect of grain size and the presence of second-phase particles on strength. According to Hall-Petch equation ( $\sigma = \sigma_i + kD^{-\frac{1}{2}}$ ) (Ref 17), strength ( $\sigma$ ) is dependent on the grain size ( $D$ ) and Orowan-Ashby equation ( $\Delta\sigma \approx k'\lambda^{-\frac{1}{2}}$ ) (Ref 17) shows that the strengthening by second-phase particles is related to interparticle spacing ( $\lambda$ ). So, grain size and interparticle spacing are decisive factors affecting the

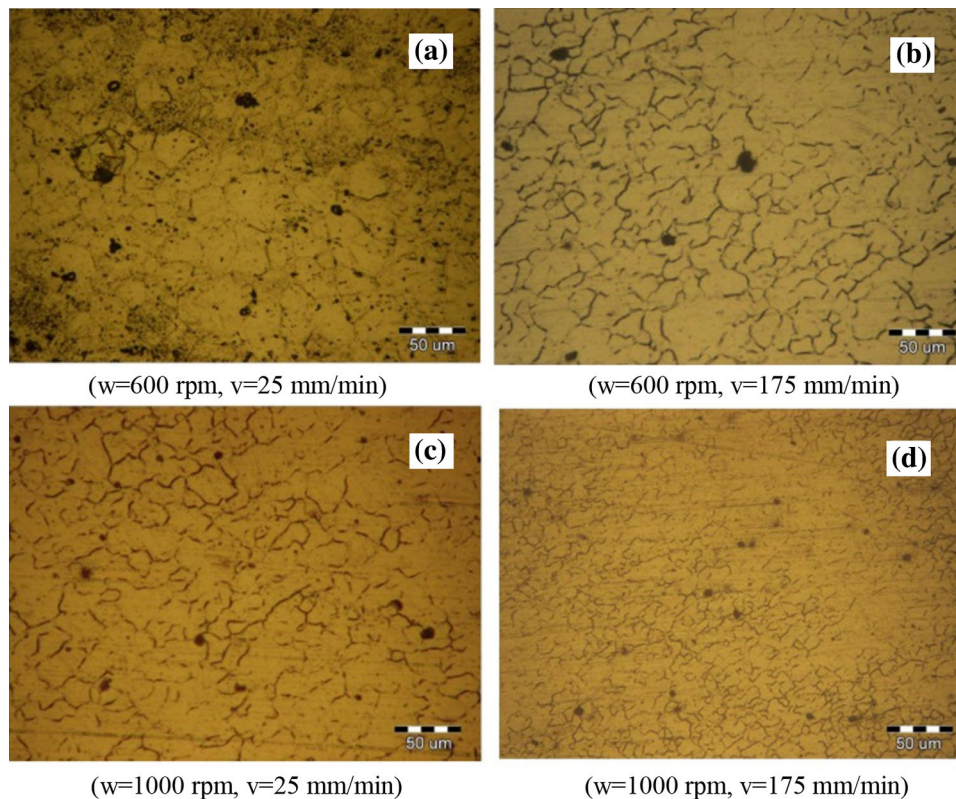


**Fig. 7** Microstructure of some samples FS welded and processed with SiC particles at different welding conditions (w and v represent the rotation and traverse speeds, respectively)

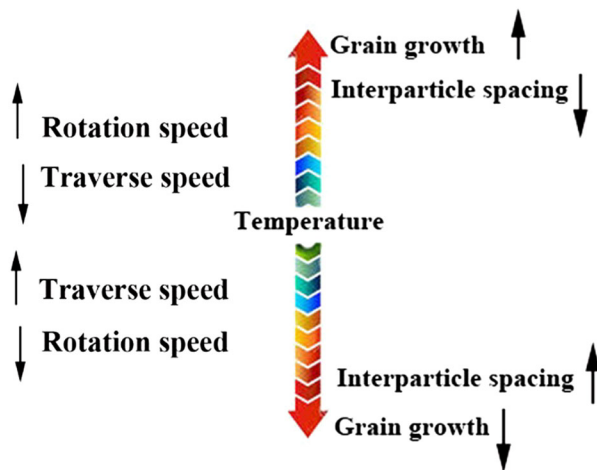


**Fig. 8** The effect of process parameters of FSW, while second-phase particles are added, on the temperature of nugget zone. The effect of temperature on grain growth and interparticle spacing is also presented (upward arrows indicate increase and downward arrows indicate decrease)

strength of FS-welded zone containing second-phase particles. When grain size and interparticle spacing are low, the strengthening is high. Additionally, ductility enhances as the grain size and interparticle spacing decrease. This relates to the transition in the fracture mechanisms from intergranular fracture to transgranular fracture as grain size decreases (Ref 18). Therefore, neither high heat input (which grain size is high) nor low heat input (which interparticle spacing is high)

does not guarantee the best mechanical properties of weld. So, arranging the process parameters in a way that grain size and interparticle spacing are low, is important and it results in high strength and ductility and low grain size.

In addition to the aforementioned affects, low and high heat input to the weld region might have other affects. Mishra et al. (Ref 19) pointed out that low heat generation in weld zone cannot soften and stir the material in the nugget zone. If the material in stir zone is too cold, then voids or other flaws may be present in the stir zone and in extreme cases the tool may break because of high forces acting on the tool. Excessively high heat input in the weld zone, on the other hand, may be detrimental to the final properties of the weld, due to the liquation of low-melting-point phases and grain growth (Ref 19).

These competing demands lead to the concept of a “processing window.” This window represents the range of processing parameters, namely tool rotation and traverse speeds, that produce a good-quality weld. Within this window, the resulting weld will have a sufficiently high heat input to ensure adequate material plasticity but not so high that the weld properties are excessively deteriorated. Although it should be pointed out that the ranges of this window for various materials are different. Based on Fig. 6, in the current work, the optimum values of rotational and traverse speeds are 800 rpm and 75 mm/min, respectively.

To study the improvement in the properties of FS-welded sample with incorporation of SiC particles, the microstructure and mechanical properties were compared with those of FS-welded sample. In both cases, FSW process was carried out under optimum welding conditions.

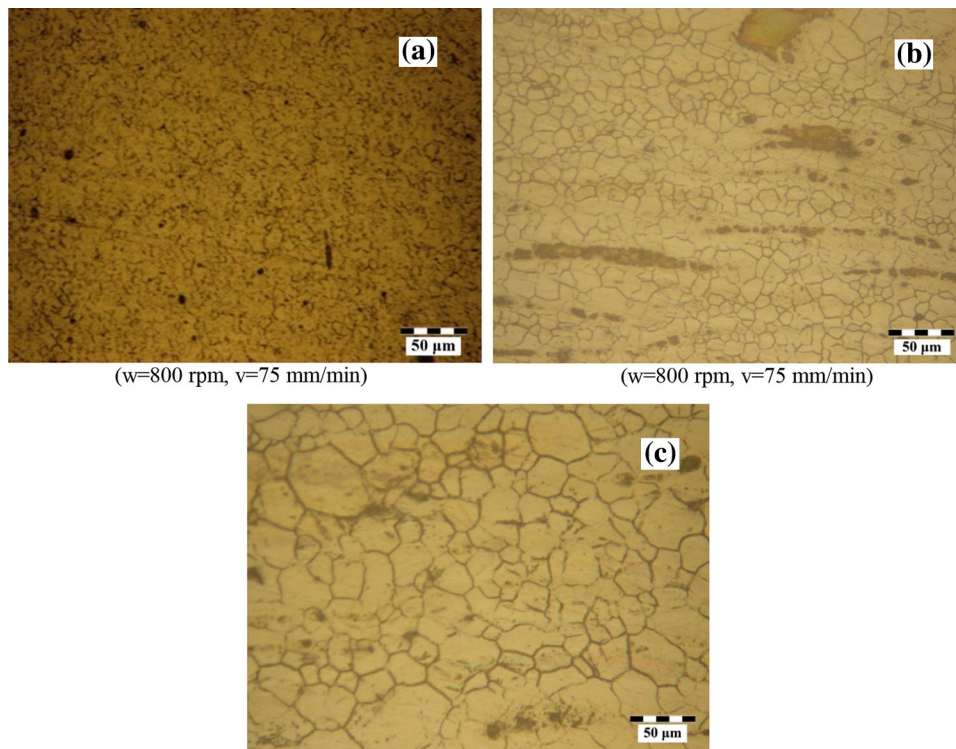


**Fig. 9** Microstructures of different samples (a) FS welded and processed with SiC particles, (b) FS welded, and (c) base material (w and v stand for rotation and traverse speeds, respectively)

The microstructures of FS-welded and processed sample, FS-welded sample, and the base material are presented in Fig. 9. It is observed that grain size of FS-welded samples is smaller than that of the base material. This can be related to the effects of dislocations which move and multiply during stirring and arrange themselves at high-angle boundaries, and consequently cell structure with small grain size is formed (Ref 15). Furthermore, it is observed in Fig. 9 that the grain size of FS-welded and processed sample with SiC particles is lower than that of FS-welded sample. As stated before, this can be related to the formation of dislocation loops around the particles which results in the constitution of cell structure with fine grains (Ref 15).

In Fig. 10, the mechanical properties of the sample FS welded and processed with SiC particles is compared with that of FS-welded sample. As it is observed, the presence of powders has increased the strength and ductility. This can be related to the role of SiC particles which act as reinforcing particles. The pinning effect of SiC particles on dislocations has been discussed by different researchers (Ref 20-22). Low grain size and the presence of second-phase particles delay the fracture and increase the ductility as they change intergranular fracture mechanism to transgranular fracture mechanism (Ref 18).

It is believed that second-phase particles act in two distinct ways to retard the motion of dislocations (Ref 17). These reinforcing particles either may be cut by the dislocations when the particles are small and soft, or resist cutting, and the dislocations are forced to bypass them while leaving a dislocation loop around each particle. In both conditions, the presence of particles hinders the movement of dislocation and leads to strengthening and high ductility (Ref 17).

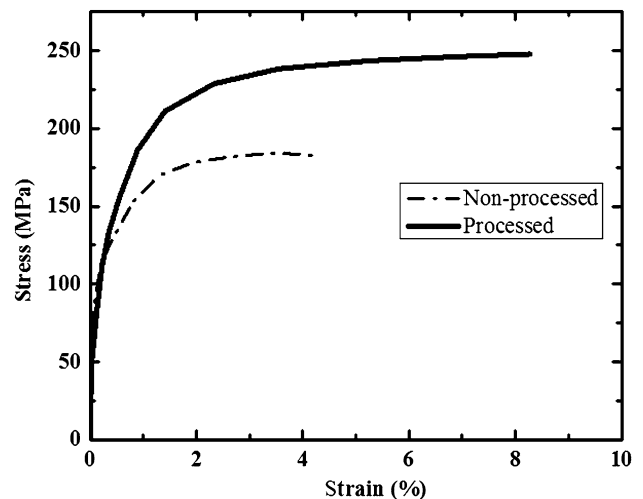


**Fig. 10** Comparison between the mechanical properties of weld processed and weld non-processed samples. For both conditions, rotation speed was 800 rpm and traverse speed was 75 mm/min

In Fig. 11, the formability index of weld sample processed by SiC particles is compared with that of non-processed sample. The formability index which is quantified by “UTS  $\times$  ductility” relation can be regarded as the ability of substance for energy absorption during deformation (Ref 23). As illustrated in this figure, the sample processed with SiC has a higher formability index with regard to the friction-stir-welded sample. This indicates that the former sample has greater capacity for deformation without being fractured.

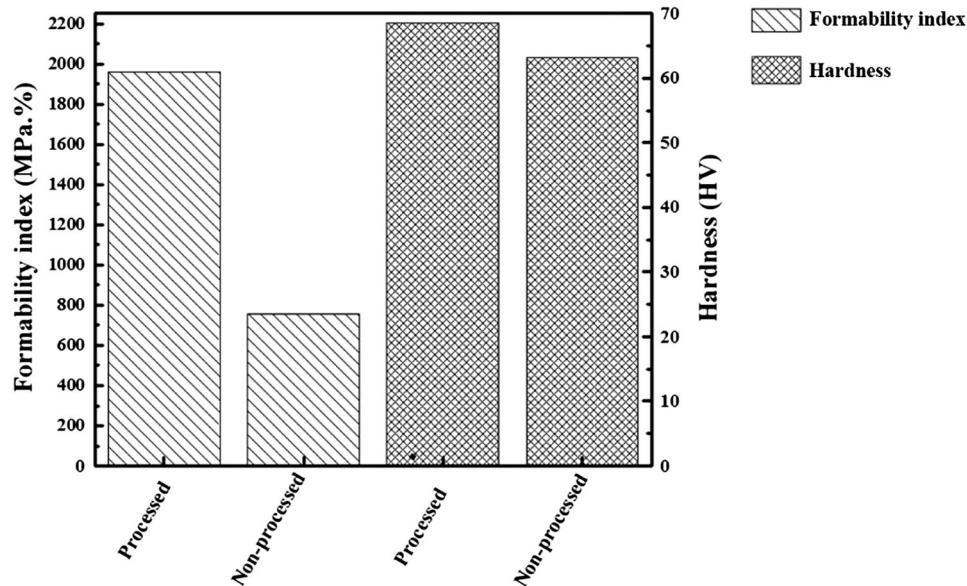


**Fig. 11** Comparison between the formability index and hardness of sample FS welded and processed with SiC particles and FS-welded sample. For both conditions, rotation speed was 800 rpm and traverse speed was 75 mm/min

Increase of hardness for the sample FS welded and processed with SiC particles with respect to the FS-welded sample is also depicted in Fig. 11. As it was stated before, this enhancement relates to the presence of SiC particles which reinforce the matrix and impede the movement of dislocations (Ref 17).

#### 4. Conclusions

Hybrid welding and processing of AZ31 magnesium alloys was carried out in the current research. SiC powders were added to the weld zone prior to FSW processing, and the resulting microstructure and mechanical properties were analyzed. These findings were compared with those of FS-welded sample. The results showed that proper welding/processing conditions led to homogenous distribution of SiC particles while grain size and interparticle spacing were low. The addition of SiC particles during stirring increased the ductility, strength, and accordingly the formability index of processed sample with respect to the FS-welded sample without SiC addition. Finally, FSW process, with SiC particles incorporated in the weld zone, is recommended to improve the mechanical properties of AZ31 magnesium alloy weld.

#### References

1. H.E. Friedrich and B.L. Mordike, *Magnesium Technology: Metallurgy, Design Data, Applications*, Springer, Berlin, 2006
2. Y. Morisada, H. Fujii, T. Nagaoka, and M. Fuukusumi, Effect of Friction Stir Processing with SiC Particles on Microstructure and Hardness of AZ31, *Mater. Sci. Eng. A*, 2006, **433**, p 50–54
3. <http://www.aircraftmaterials.com/data/magnesium/az31b.html>
4. W.B. Lee, J.W. Kim, Y.M. Yeon, and S.B. Jung, The Joint Characteristics of Friction Stir Welding AZ91D Magnesium Alloy, *Mater. Trans.*, 2003, **44**, p 917–923

5. F. Czerwinski, *Magnesium Alloys: Design, Processing and Properties*, InTech Publishing, Croatia, 2011
6. P. Kurtyka, I. Sulima, W. Wojcicka, N. Rylko, and A. Pietras, The Influence of Friction Stir Welding Process on Structure and Mechanical Properties of the AlSiCu/SiC Composites, *J. Achiev. Mater. Manuf. Eng.*, 2012, **55**, p 339–344
7. P.V. Kumar, G.M. Reddy, and K.S. Rao, Microstructure and Pitting Corrosion of Armor Grade AA7075 Aluminum Alloy Friction Stir Weld Nugget Zone-Effect of Post Weld Heat Treatment and Addition of Boron Carbide, *Def. Technol.*, 2015. doi:10.1016/j.dt.2015.01.002
8. Y. Huang, T. Wang, W. Guo, L. Wan, and S. Lv, Microstructure and Surface Mechanical Property of AZ31/SiC Surface Composite Fabricated by Direct Friction Stir Processing, *Mater. Des.*, 2014, **59**, p 274–278
9. H. Zhang, S.B. Lin, L. Wu, and J.C. Feng, Microstructural Studies of Friction Stir Welded AZ31 Magnesium Alloy, *Acta Metall. Sin.*, 2004, **17**, p 747–753
10. P. Karthikeyan and K. Mahadevan, Investigating on the Effects of SiC Particles Addition in the Weld Zone During Friction Stir Welding of Al 6351 Alloy, *Int. J. Adv. Manuf. Technol.*, 2015. doi:10.1007/s00170-015-7160-9
11. Y.F. Sun and H. Fujii, The Effect of SiC Particles on the Microstructure and Mechanical Properties of Friction Stir Welded Pure Copper Joints, *Mater. Sci. Eng. A*, 2011, **528**, p 5470–5475
12. ASTM E112–13, *Standard Test Methods for Determining Average Grain Size*, ASTM International, West Conshohocken, 2013
13. ASTM E8, E8 M-15, *Standard Test Methods for Tension Testing of Metallic Materials*, ASTM International, West Conshohocken, 2015
14. ASTM E384–11e1, *Standard Test Method for Knoop and Vickers Hardness of Materials*, ASTM International, West Conshohocken, 2011
15. D. Hull and D.J. Bacon, *Introduction to Dislocations*, 5th ed., Elsevier, New York, 2011
16. M. Abbasi, B. Bagheri, and R. Keivani, Thermal Analysis of Friction Stir Welding Process and Investigation into Affective Parameters Using Simulation, *J. Mech. Sci. Technol.*, 2015, **29**, p 861–866
17. G.E. Dieter and D. Bacon, *Mechanical Metallurgy*, McGraw-Hill, London, 1988
18. T. Mukai, T. Mohri, M. Mabuchi, M. Nakamura, K. Ishikawa, and K. Higashi, Experimental Study of a Structural Magnesium Alloy with High Absorption Energy Under Dynamic Loading, *Scripta Mater.*, 1998, **39**, p 1249–1253
19. Y.Z. Estrin, P.A. Zabrodin, I.S. Braude, T.V. Grigorova, N.V. Iasev, V.V. Pustovalov, V.S. Fomenko, and S.E. Shumilin, Low-Temperature



- Plastic Deformation of AZ31 Magnesium Alloy with Different Microstructures, *Low Temp. Phys.*, 2010, **36**, p 1100–1106
20. R.S. Mishra, P.S. De, and N. Kumar, *Friction Stir Welding and Processing: Science and Engineering*, Springer, London, 2014
  21. M. Dadaei, H. Omidvar, B. Bagheri, M. Jahazi, and M. Abbasi, The Effect of SiC/Al<sub>2</sub>O<sub>3</sub> Particles Used During FSP on Mechanical Properties of AZ91 Magnesium Alloy, *Int. J. Mater. Res.*, 2014, **105**, p 369–374
  22. J. Guo, B.Y. Lee, C.N. Sun, G. Bi, and J. Wei, Effect of Nano-particle Addition on Grain Structure Evolution of Friction Stir Processed Al 60 61 During Post-Weld Annealing, *2015 TMS Annual Meeting & Exhibition*, Orlando, USA
  23. M. Naderi, M. Abbasi, and A. Saeed-Akbari, Enhanced Mechanical Properties of a Hot-Stamped Advanced High-Strength Steel Via Tempering Treatment, *Met. Mater. Trans. A*, 2014, **44**, p 1852–1861